Chemical Geology 285 (2011) 115–123

Contents lists available at ScienceDirect

Chemical Geology

journal homepage: www.elsevier.com/locate/chemgeo

Proton binding of bacterial exudates determined through potentiometric titrations

Lindsay A. Seders *, Jeremy B. Fein

University of Notre Dame, Department of Civil Engineering and Geological Sciences, 156 Fitzpatrick Hall, Notre Dame, IN 46556, USA

ARTICLE INFO

Article history:
Received 23 September 2010
Received in revised form 23 March 2011
Accepted 26 March 2011
Available online 3 April 2011

Editor: J.D. Blum

Keywords:
Bacterial exudates
Potentiometric titrations
Natural organic acids

ABSTRACT

Bacterial exudates can play a role in metal reduction and mineral dissolution. Exudates were collected from non-metabolizing Gram-positive (*Bacillus subtilis*) and Gram-negative (*Shewanella oneidensis*) bacterial species by suspending and rotating 40, 80, or 100 g (wet mass)/L bacteria in $NaClO_4$ solutions of 0.01, 0.1, or 0.3 M for 2.5 h, and removing the cells by centrifugation. Exudate solutions were analyzed for total organic carbon concentrations, which varied as a function of bacterial type and concentration. However, FTIR spectra of all exudate samples were essentially identical under all experimental conditions. Potentiometric titrations of the exudate solutions were conducted for each of the bacterial concentrations and ionic strength conditions examined, for both of the bacterial species. Both 'up-pH' and 'down-pH' titrations were conducted to determine the extent of reversibility of the proton binding reactions, and titration data were modeled using a discrete-site modeling approach to determine the number of discrete proton-active functional groups required to account for the observed buffering capacity and to place quantitative constraints on values of the acidity constants and site concentrations for the proton binding sites. A 3-site model fit the titration data the best, and the calculated acidity constant values did not vary significantly as a function of bacterial species studied, ionic strength, or quantity of biomass used to generate the exudate solution. The calculated site concentrations varied with ionic strength and bacterial species. *B. subtilis* exudates showed a decrease in total site concentrations with increasing ionic strength, and *S. oneidensis* showed an increase with increasing ionic strength; however, the range of total site concentrations was similar for both species. Total buffering capacities and site concentrations for the exudates were approximately one order of magnitude lower than those previously determined for bacterial cells per gram of bacteria but were within the ranges of those calculated for EPS and humic substances.

1. Introduction

Bacteria play an important role in many environmental processes including adsorption and/or reduction of metals (e.g., Beveridge and Murray, 1976; Lovely, 1993; Brown and Parks, 2001; Newman and Banfield, 2002; Borch et al., 2010); precipitation or dissolution of minerals (e.g., Fortin and Beveridge, 1997; Bennett et al., 2001); and the degradation of natural organic matter and certain anthropogenic contaminants (e.g., Young et al., 2005; Mrozik and Piotrowska-Seget, 2010; Tiquia, 2010). Most of these processes involve the bacterial cell wall and/or bacterial metabolism directly. However, bacteria, through active metabolic processes or through lysis and decay, exude a wide range of organic molecules, and there is growing evidence that these bacterial exudates also can contribute to important geochemical processes. For example, metal reduction can occur in the presence of bacterial exudates, as in the case of Pu(VI) reduction to Pu(V) by *Bacillus subtilis* exudates (Ohnuki et al., 2007). In addition, bacterial exudates have been shown to accelerate mineral dissolution rates and to increase the extent of dissolution (Lee and Fein, 2000; Perry et al., 2003, 2005; Pokrovsky et al., 2009). The exudates in these studies are dissolved organic molecules exuded from whole cells and are not the same as the non-aqueous extracellular polymeric substances (EPS) which are often produced by bacteria and are an important component of biofilms. The observed effects of the bacterial exudates suggest that they contain proton-active organic acid functional groups as these are the most likely means of interacting with metals and mineral surfaces.

Despite the indications that bacterial exudates can affect geochemical processes, there has been virtually no work conducted to quantify their environmental concentrations or characteristics. The objective of this study is to use FTIR spectrometry to provide an initial qualitative description of the exudate molecules and to use potentiometric titrations to determine if the molecules contain proton binding sites and to characterize the acidity constants and the concentrations of those sites. Exudates are defined here as dissolved bacterial material from the cell surface and/or material from the cell cytoplasm which enters solution as a result of cell lysis or passive excretion. No effort is made here to differentiate amongst the different components, as all of these types of molecules are likely to be present in natural systems. We studied the exudates from a Gram-positive and a Gram-negative

* Corresponding author at: Present address: Southern Methodist University, Department of Civil and Environmental Engineering, P.O. Box 750340, Dallas, TX 75275-0340, USA.
E-mail address: Lseders@smu.edu (L.A. Seders).

0009-2541/$ – see front matter © 2011 Elsevier B.V. All rights reserved.
doi:10.1016/j.chemgeo.2011.03.017

bacterial species to better understand how the differences in cell wall characteristics may influence the properties of bacterial exudates, and we examined the exudates produced at different bacterial concentrations and ionic strengths in order to determine the effects of changing solution chemistry on the production of bacterial exudates and to better constrain our thermodynamic modeling. The results represent a framework for understanding the effects of bacterial exudates on geochemical processes and provide a basis for quantitative modeling of metal interactions with the proton-active sites within the exudates. We use the results to compare the proton binding behavior of bacterial exudates with that of bacterial cells, as well as with that of EPS and humic substances.

2. Materials and methods

2.1. Experimental

2.1.1. Bacterial growth and exudate preparation

The bacterial species used in these experiments were the aerobic, Gram-positive soil bacterium *Bacillus subtilis* and the facultatively anaerobic, Gram-negative bacterium *Shewanella oneidensis* MR-1, originally collected from lake sediment. The cell wall constituents and reactivity of *B. subtilis* (Beveridge and Murray, 1980; Fein et al., 2005) and *S. oneidensis* (Venkateswaran et al., 1999; Ha et al., 2010; Mishra et al., 2010) have been well characterized. *B. subtilis* and *S. oneidensis* were initially grown aerobically in 3 mL of trypticase soy broth (TSB) spiked with 0.5% yeast extract (YE) at 32 °C with shaking for 24 h. Bacteria were then transferred to 2 L of the TSB/YE solution to grow under the same conditions and harvested after 24 h once reaching the stationary growth phase. The washing procedure consisted of centrifugation at 8500 rpm, followed by resuspension of the cells in a $NaClO_4$ solution of the desired ionic strength, repeated five times.

The exudate solutions were prepared by suspending bacteria in a $NaClO_4$ solution of the same ionic strength with which they were washed, allowing the bacteria to soak for 2.5 h, and separating the bacterial cells by centrifugation (for images of the cells removed during centrifugation see Figure S1). Although it is possible that some of the exuded organics were colloidal, we refer to them as dissolved and define that to include all material in the supernatant that is not removed by our centrifugation step. Exudate solutions were made from bacterial suspensions of either *B. subtilis* or *S. oneidensis* in 0.01 and 0.1 M $NaClO_4$ at 40, 80, and 100 g/L bacteria (wet mass) and in 0.3 M $NaClO_4$ at 100 g/L (wet mass). Each bacterial suspension was adjusted to pH 5.5 using aliquots of 6 M HNO_3 and rotated for 2.5 h, with pH readjusted every 30 min. After rotating for 2.5 h, the bacterial suspension was centrifuged at 10,000 rpm for 10 (*B. subtilis*) or 20 min (*S. oneidensis*) to remove the bacterial cells. The centrifuge times differed for the two bacterial species because the *S. oneidensis* supernatant still contained visible non-dissolved components after 10 min, whereas the *B. subtilis* supernatant had become clear. Thus, a longer centrifuge time was deemed necessary for *S. oneidensis*; after centrifuging for 20 min, the *S. oneidensis* supernatant also became clear. After the bacteria were removed from their electrolyte soaking solutions via centrifugation, the remaining supernatant contained bacterial material from the cell surface and/or material from the cell cytoplasm which entered solution as a result of cell lysis or passive excretion. No effort was made to determine the exact location on and/or in the bacterial cells that was the source for these materials. The supernatant or 'exudate' solution was decanted and used to conduct potentiometric titrations. A portion of the exudate solution was also diluted for measurements of the total organic carbon concentration ([TOC]) (Shimadzu TOC-V), and the remaining solution was frozen and then freeze dried for FTIR analysis (Bruker Tensor 27 with Platinum ATR). FTIR spectra were baseline corrected and normalized to the height of the 1090–1062 cm^{-1} peak to account for variations in the strength of the absorbance of each sample.

2.1.2. Potentiometric titrations

Potentiometric titrations were conducted on the exudate solutions with a Radiometer Analytical ABU91 titrator. The automated burette assembly added aliquots of 1.041 N HCl or 1.030 N NaOH (Sigma-Aldrich; St. Louis, MO) with a potentiometric stability of 0.01 mV/s required between additions. Each exudate solution was first acidified to pH 2.5. A forward or 'up-pH' titration was then conducted by basifying to pH 10, and the pH and volume of base added were recorded at each step. Similarly, a reverse or 'down-pH' titration was conducted for each solution by acidifying back to pH 2.5, again recording pH and volume of acid added at each step. Four NIST-standard pH buffer solutions (pH 1.68, 4.01, 7.00, and 10.00) were used to calibrate the change measured by the electrode after each acid or base addition (in mV) to pH units. Prior to each titration, the exudate solution was purged with N_2 gas for at least 30 min to remove dissolved CO_2, and titrations were conducted in a closed polypropylene titration vessel into which N_2 gas was continuously supplied to the headspace to further exclude atmospheric CO_2. A small, Teflon-coated magnetic stir bar continuously stirred the solutions throughout the titration. Titrations of a given exudate solution were conducted in duplicate, and each set of conditions (ionic strength, bacterial type, and bacterial concentration) was examined in at least duplicate (i.e., from at least two separate bacterial batches).

In order to compare our exudate titration data with titration data previously collected for bacterial cells, the titration results were normalized and presented as

$$(C_a - C_b) / (\text{g/L bacteria}) \quad (1)$$

where C_a is the total concentration of acid added to the system and C_b is the total concentration of base added, both in moles per L. (g/L bacteria) represents the concentration of bacteria that was used to generate the exudate solution in question (g of bacteria, wet mass, per L solution). The total buffering capacity of each exudate solution (in moles per g bacteria) over the pH range of 3 to 9 was also calculated from the titration data for comparison purposes by subtracting the value of $(C_a - C_b)/(\text{g/L bacteria})$ at pH 9 from its value at pH 3.

The exudate titration data were also normalized for comparison to data collected previously for EPS and for humic substances according to the following expression:

$$(C_a - C_b) / (\text{g/L exudate}) \quad (2)$$

where (g/L exudate) is the concentration of exudate (g of exudate per L solution) in the electrolyte solution, as determined by direct measurement of dissolved mass in control exudate solutions. These controls were generated for both *B. subtilis* and *S. oneidensis* from 80 g/L bacterial suspensions in 0.1 M $NaClO_4$. A known volume of each control exudate solution was placed into a test tube and then freeze-dried, followed by drying overnight in an oven at 50 °C. The mass of the HNO_3 that was used to adjust the pH of the suspension was explicitly included in the calculations of the exudate mass. Triplicate samples were prepared in this manner for exudate solutions for each bacterial species. In addition, an exudate-free background solution was treated in the same manner to determine the contribution of $NaClO_4$ to the dry exudate mass. For the comparisons to EPS and humic substances, the total buffering capacity of each exudate solution (in moles of sites per g exudate) was calculated over the pH range of 4 to 9 by subtracting the value of $(C_a - C_b)/(\text{g/L exudate})$ at pH 9 from its value at pH 4. The uncertainties associated with the calculated buffering capacities that we report are 1 σ errors calculated using an $n-1$ standard deviation equation from forward and reverse replicate titrations collected under the same experimental conditions.

2.2. Chemical equilibrium modeling

Chemical equilibrium modeling was conducted using FITEQL 2.0 (Westall, 1982) with a discrete site model of the reactivity of the bacterial exudate functional groups. Potentiometric titration experiments are essentially proton adsorption measurements, but they are conducted in systems in which it is impossible to keep track of the total absolute concentration of H as one might do with a bulk metal adsorption experiment (Westall et al., 1995; Fein et al., 2005). Therefore, instead of constraining the calculations using a mass balance on the total absolute H concentration, modeling of potentiometric titration data uses a mass balance on the excess/deficit of protons associated with the titrated molecules relative to an arbitrarily defined zero proton condition. In this study, in parallel with potentiometric titration experiments involving bacterial suspensions (e.g., Fein et al., 2005), we define the zero proton condition as that at which the binding sites on the bacterial exudates are fully protonated. We model the proton buffering behavior of the exudate molecules as simple organic acid functional group sites, where the deficit of protons is represented as:

$$R{-}L_iH^0 \leftrightarrow R{-}L_i^- + H^+ \quad (3)$$

where L_i represents a proton-active functional group type, and R represents the exudate molecule to which the functional groups are attached. The equilibrium constant for Reaction (3), termed the acidity constant, is expressed as:

$$K_{a(i)} = \frac{a_{R-L_i^-}\, a_{H^+}}{a_{R-L_iH^0}} \quad (4)$$

where *a* represents the activity of the subscripted component in solution, and activity coefficients of neutral species are assumed to be 1. Equilibrium constants for the dissociation of water and sodium hydroxide were obtained from Martell and Smith (2001). Activity coefficients for ionic aqueous species were calculated using the Davies equation within FITEQL (Westall, 1982).

The potentiometric titration data were used to solve for the $pK_{a(i)}$ values, as well as for the concentrations of each site type, *i*. The calculated site concentrations were normalized to the initial bacterial concentration in g per L used to generate each exudate solution, as well as to g exudate per L solution. For comparison purposes, the total site concentration was calculated for each dataset and averaged for each experimental condition. Models with 1 to 5 discrete proton binding site types were tested for their fits to the model data. The goodness-of-fit of each model for each titration dataset was determined based upon the calculated variance parameter, V(Y), as calculated by the FITEQL program. A V(Y) value of 1 indicates a perfect fit, with values much greater than 1 indicating an inappropriate model and values much less than 1 indicating a model with too many adjustable parameters; values from 0 to 20 can be considered good fits (Westall, 1982).

3. Results and discussion

3.1. Exudate solutions

B. subtilis exudate solutions were clear and colorless; *S. oneidensis* exudate solutions were also clear but with a reddish-orange color, which darkened with increasing initial bacteria concentration. During purging with N_2 gas, *B. subtilis* solutions became much frothier than *S. oneidensis* solutions. These differences could result from differences in composition as well as differences in the concentration of material in solution. Changes in the total organic carbon concentration [TOC] of the exudate solutions under the range of experimental conditions are shown in Fig. 1. Compared to *B. subtilis* exudate solutions, *S. oneidensis* solutions were lower in [TOC] (by at least half) under all conditions,

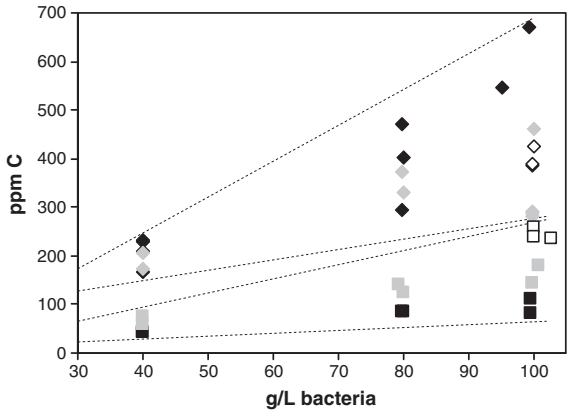

Fig. 1. Bacterial exudate TOC data. Measured [TOC] (ppm C) as a function of the initial *B. subtilis* (diamonds) or *S. oneidensis* (squares) concentration at 0.01 M (black), 0.1 M (gray), or 0.3 M (white) $NaClO_4$. The dashed lines separate the field for the *B. subtilis* data (top) from the field for the *S. oneidensis* data (bottom).

and [TOC] values increased with increasing initial bacterial concentration. There does not appear to be a significant [TOC] dependence on ionic strength. Qualitatively, the FTIR spectra of the freeze-dried exudate solutions (Fig. 2) were similar for both bacterial types. The same major peaks were present in samples of exudate solutions from both bacterial species, and although there are some differences as a function of ionic strength, there is no consistent ionic strength dependence. The position of the peaks also does not vary significantly

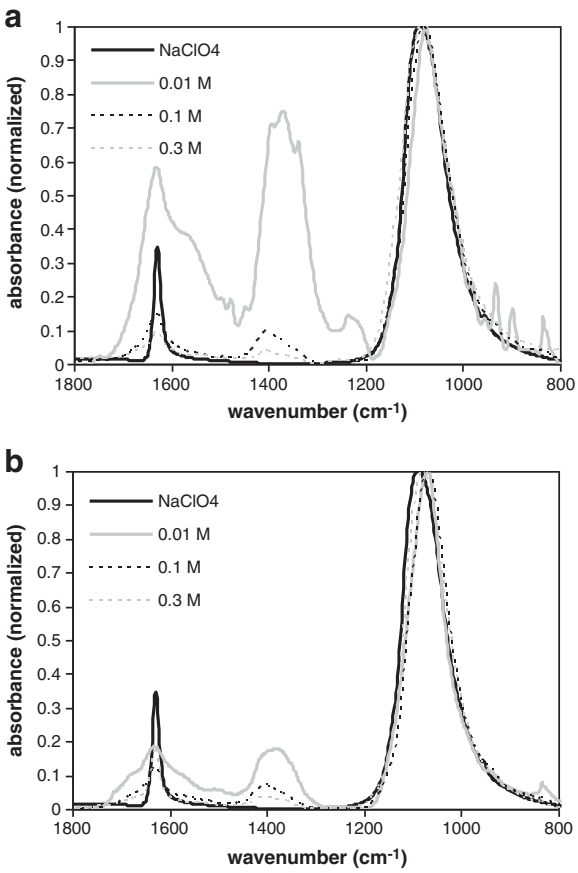

Fig. 2. Bacterial exudate FTIR. FTIR spectra of a) *B. subtilis* and b) *S. oneidensis* 100 g/L exudate solutions. The black line is pure $NaClO_4$ and the exudates made in 0.01 M, 0.1 M, and 0.3 M $NaClO_4$ are represented by the gray, black dashed, and gray dashed lines, respectively.

as a function of ionic strength or initial bacterial concentration. These bacterial exudate spectra have a strong group of peaks in the range of 1467–1276 cm^{-1} which are indicative of polysaccharides, as are the peaks at 933, 898, and 835 cm^{-1} (e.g., Brandenburg and Seydel, 1996; Yang and Zhang, 2009). The peaks at 1635 and 1580 cm^{-1} have been assigned to Amide I and Amide II, respectively, and FTIR spectra of bacterial cell walls and cell wall fragments also show Amide I and II peaks from the bacterial membrane proteins (e.g., Haris and Chapman, 1996; Jiang et al., 2004). However, the exudate spectra differ in that their polysaccharide peaks from 1467–1276 cm^{-1} are much stronger than those of bacterial cell walls (e.g., Naumann et al., 1996; Jiang et al., 2004).

3.2. Exudate titrations

Forward and reverse titrations of both *B. subtilis* and *S. oneidensis* exudate solutions (Figs. 3 and 4) showed full reversibility of the proton binding reactions on the timescale of the experiments. Experimental replicates from the same exudate solution, as well as from exudate solutions made at the same conditions but from a different bacterial batch, also generally showed good agreement (data not shown). The bacterial exudates exhibited a significant buffering capacity over the pH range examined in this study (2.5–10). In order to compare the buffering capacity of bacterial exudates to that typically exhibited by bacterial cells, the total buffering capacity of the exudate solutions from pH 3 to 9 was averaged for each combination of bacterial type, bacterial concentration, and ionic strength and compared to the total buffering capacity over the same pH range from potentiometric titrations performed previously on *B. subtilis* (Fein et al., 2005) and *S. oneidensis* (Mishra et al., 2010) bacterial cell suspensions (Table 1). This comparison is meaningful because the buffering capacity of the exudate solutions was normalized to the mass of bacteria used to generate those solutions, so the comparison relates the buffering capacity of a cell suspension to the buffering capacity of the exudate solution generated by that same concentration of cells.

The mass normalized buffering capacities of the exudate solutions in this study were fairly close to one another, ranging from 2.75 to 7.83×10^{-5} mol/g. The exudate buffering capacities were approximately an order of magnitude lower than those exhibited by *B. subtilis* (1.6–2.8×10^{-4} mol/g) and *S. oneidensis* (3.1×10^{-4} mol/g), as well as the wide range of bacteria compared by Borrok et al. (2005). The buffering capacities of the exudate solutions made from different bacterial concentrations at a given ionic strength showed a slight decrease with increasing bacterial concentration in most cases (e.g., the total buffering capacity of the *B. subtilis* exudate decreased from $6.02\pm0.32\times10^{-5}$ mol/g at 40 g/L to $3.85\pm0.42\times10^{-5}$ mol/g at 100 g/L, and the *S. oneidensis* exudate capacity decreased from $5.97\pm0.39\times10^{-5}$ mol/g at 40 g/L to $4.43\pm0.50\times10^{-5}$ mol/g at 100 g/L).

There were also significant changes in buffering capacity with increasing ionic strength, although the effects varied from one species to the other. The total buffering capacity of the *B. subtilis* exudates decreased with increasing ionic strength (e.g., from $7.25\pm0.60\times10^{-5}$ mol/g at 0.01 M to $3.85\pm0.42\times10^{-5}$ mol/g at 0.1 M to $2.75\pm0.24\times10^{-5}$ mol/g at 0.3 M in the 100 g/L exudate solutions). The reverse was true for the *S. oneidensis* exudates with total buffering capacity increasing significantly with increasing ionic strength (e.g., from $3.04\pm0.46\times10^{-5}$ mol/g at 0.01 M to $4.43\pm0.50\times10^{-5}$ mol/g at 0.1 M to $6.00\pm0.45\times10^{-5}$ mol/g at 0.3 M in the 100 g/L exudate solutions). However, the buffering capacities for *B. subtilis* and *S. oneidensis* exudates covered essentially the same range, and total buffering capacity at 0.1 M was similar for the exudates from both bacterial species. In titrations conducted with whole but non-metabolizing *B. subtilis* bacterial cells (Fein et al., 2005), the effect of changing ionic strength on total buffering capacity was small relative to the experimental uncertainties. Titrations conducted on cells of the algal species *Pseudokirchneriella subcapitata* in 0.1 M $NaClO_4$ (Kaulbach et al., 2005) showed a total buffering capacity (~3.7×10^{-5} mol/g) that was within the range calculated for our bacterial exudates.

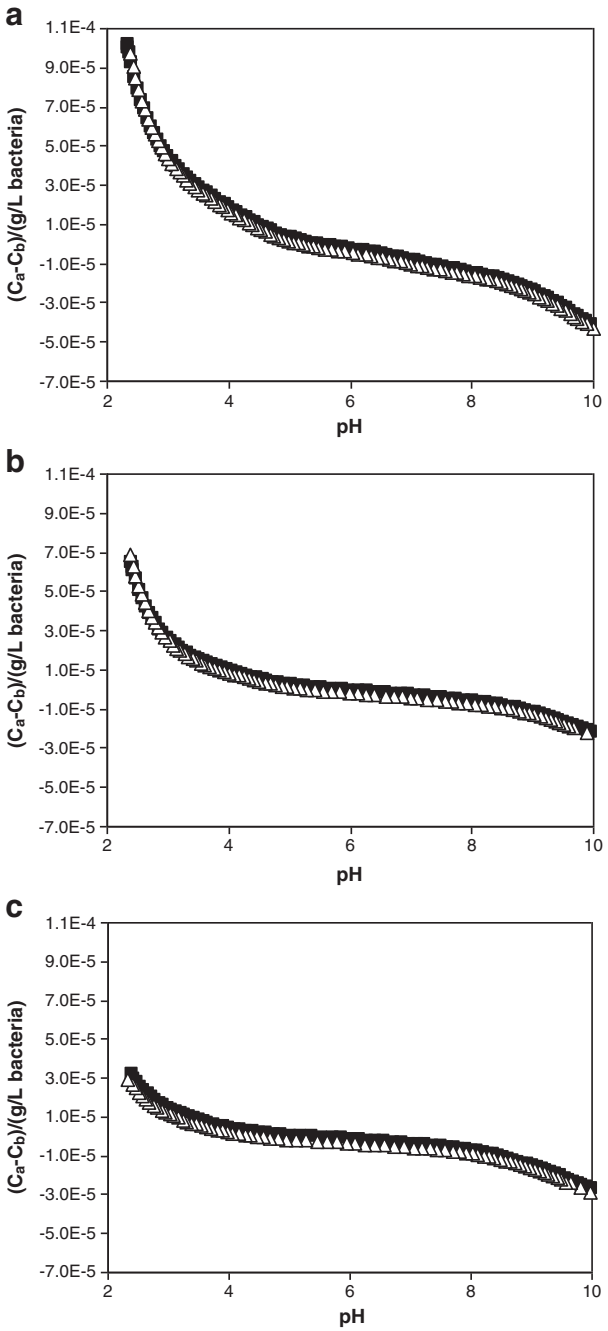

Fig. 3. *B. subtilis* exudate titrations. Representative examples of forward (black squares) and reverse (white triangles) potentiometric titration data from exudate solutions made using 100 g/L *B. subtilis* (normalized per g/L bacteria) and a) 0.01 M, b) 0.1 M, or c) 0.3 M $NaClO_4$.

3.3. Titration modeling

Based upon the calculated V(Y) values, the 1- and 2-site models were deemed inappropriate with average V(Y) values of 590 and 73, respectively. Similarly, the 4-site model showed no significant improvement in fit over the 3-site model and would not converge under some experimental conditions, and the 5-site model failed to converge in all cases. Thus, the 3-site model (average V(Y) of 6.5) was determined to be the most appropriate under all experimental conditions (e.g., Fig. 5). The calculated $pK_{a(i)}$ values (negative log $K_{a(i)}$

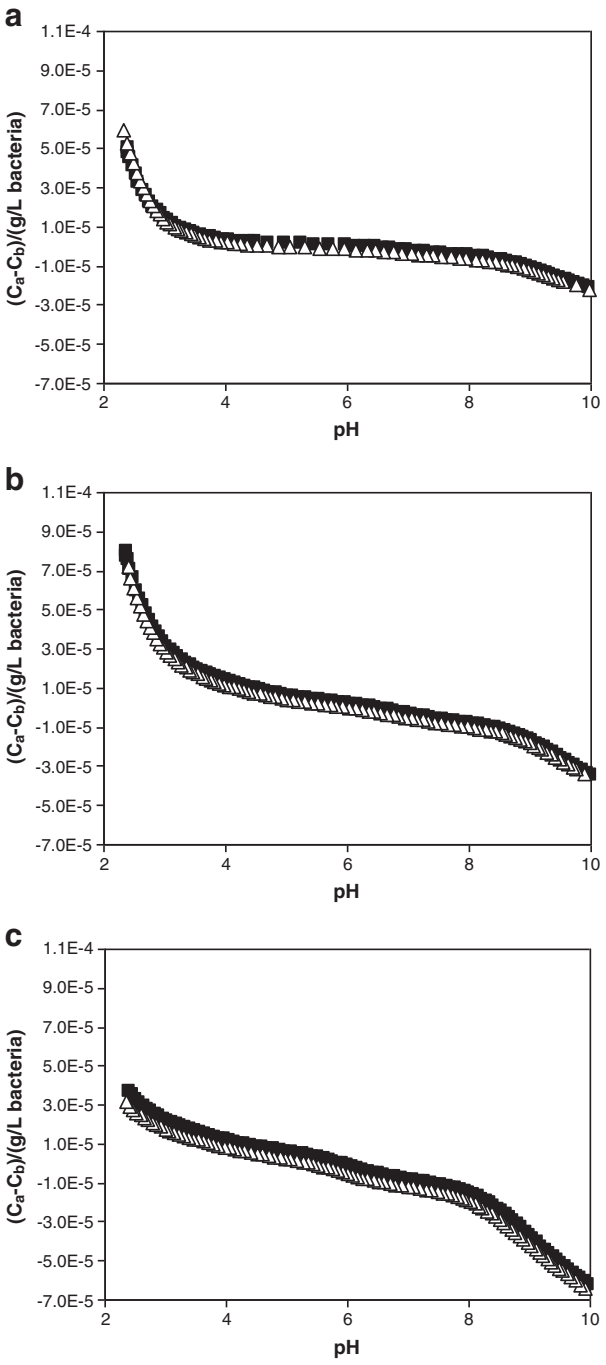

Fig. 4. *S. oneidensis* exudate titrations. Forward (black squares) and reverse (white triangles) potentiometric titration data from exudate solutions made using 100 g/L *S. oneidensis* (normalized per g/L bacteria) and a) 0.01 M, b) 0.1 M, or c) 0.3 M $NaClO_4$.

values for Reaction (4)) and site concentrations for the forward titrations do not vary significantly from the corresponding values calculated for the reverse titrations within 1 σ error. Table 2 shows a representative example of the relationship between the calculated values from the forward and reverse titrations for all replicates of a single experimental condition (100 g/L *B. subtilis* exudate in 0.1 M $NaClO_4$), and Tables S1 and S2 provide full comparisons of forward and reverse averages. Thus, the protonation reactions are fully reversible on the timescale of these experiments, and both the forward and reverse titrations reflect equilibrium conditions. Because of the lack of systematic difference between the forward and reverse titrations, we combine the results of both forward and reverse titrations from all replicates of each experimental condition to calculate average modeling parameters and their corresponding 1 σ errors (Figs. 6–8; Tables S1 and S2).

Table 1
Total buffering capacity (mol/g) of bacterial exudates and bacterial cells, calculated for the pH range of 3 to 9.

Bacterial exudates[a]	Total buffering capacity
B. subtilis	
0.01 M, 40 g/L	$7.83 \pm 0.46 \times 10^{-5}$
0.01 M, 80 g/L	$5.57 \pm 1.11 \times 10^{-5}$
0.01 M, 100 g/L	$7.25 \pm 0.60 \times 10^{-5}$
0.1 M, 40 g/L	$6.02 \pm 0.32 \times 10^{-5}$
0.1 M, 80 g/L	$4.36 \pm 0.26 \times 10^{-5}$
0.1 M, 100 g/L	$3.85 \pm 0.42 \times 10^{-5}$
0.3 M, 100 g/L	$2.75 \pm 0.24 \times 10^{-5}$
S. oneidensis	
0.01 M, 40 g/L	$4.55 \pm 0.16 \times 10^{-5}$
0.01 M, 80 g/L	$3.20 \pm 0.19 \times 10^{-5}$
0.01 M, 100 g/L	$3.04 \pm 0.46 \times 10^{-5}$
0.1 M, 40 g/L	$5.97 \pm 0.39 \times 10^{-5}$
0.1 M, 80 g/L	$4.82 \pm 0.35 \times 10^{-5}$
0.1 M, 100 g/L	$4.43 \pm 0.50 \times 10^{-5}$
0.3 M, 100 g/L	$6.00 \pm 0.45 \times 10^{-5}$
Bacterial cells	**Total buffering capacity**
B. subtilis[b]	
0.01 M, 75–150 g/L	1.6×10^{-4}
0.1 M, 75–150 g/L	2.8×10^{-4}
0.3 M, 75–150 g/L	2.3×10^{-4}
S. oneidensis[c]	
0.1 M, 50 g/L	3.1×10^{-4}

[a] This paper.
[b] Fein et al. (2005).
[c] Mishra et al. (2010).

The average $pK_{a(i)}$ values and site concentrations for the *B. subtilis* and *S. oneidensis* exudates are all within 1 σ error when compared as a function of the initial bacterial concentration. Increasing the initial bacterial concentration should increase the concentration of exudate in solution without changing its composition; thus, normalizing the site concentrations to the initial bacterial concentration, as was done here, should remove any variability due to the initial bacterial concentration, which does appear to be the case (Figs. 7 and 8).

The average $pK_{a(i)}$ values calculated for the *B. subtilis* and *S. oneidensis* exudate solutions of varying ionic strength (Fig. 6; Tables S1 and S2) are all within 1 σ error at the three $pK_{a(i)}$ values, except for the 0.3 M solutions at 100 g/L which exhibit slightly, but significantly, different $pK_{a(1)}$ values

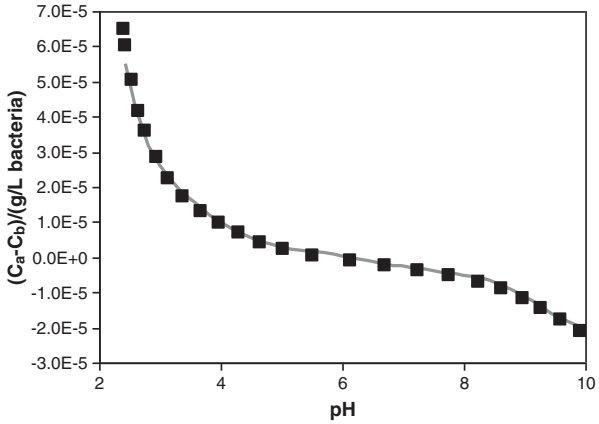

Fig. 5. 3-site model fit. Representative fit of a 3-site model (gray curve) to the potentiometric titration data (squares) for the exudate solution made using 100 g/L *B. subtilis* in 0.1 M $NaClO_4$. Some titration data points have been removed for visualization purposes.

Table 2
Calculated $pK_{a(i)}$ values and site concentrations (mol/g) from the 3-site model using forward and reverse data from potentiometric titrations on exudate solutions made with 100 g/L *B. subtilis* in 0.1 M $NaClO_4$.

Exudate titration	$pK_{a(1)}$	[Site 1]	$pK_{a(2)}$	[Site 2]	$pK_{a(3)}$	[Site 3]	V(Y)
Forward 1a	4.0	1.42×10^{-5}	6.5	4.57×10^{-6}	9.2	1.54×10^{-5}	6.81
Forward 1b	4.0	1.38×10^{-5}	6.7	4.80×10^{-6}	9.2	1.51×10^{-5}	5.97
Forward 2a	4.0	1.61×10^{-5}	6.5	5.11×10^{-6}	9.2	1.62×10^{-5}	8.40
Forward 2b	4.0	1.57×10^{-5}	6.6	5.15×10^{-6}	9.3	1.60×10^{-5}	7.78
Forward 3a	4.1	1.59×10^{-5}	6.6	5.75×10^{-6}	9.3	1.74×10^{-5}	8.06
Forward 3b	4.1	1.54×10^{-5}	6.6	5.78×10^{-6}	9.3	1.78×10^{-5}	7.70
Forward 4a	3.8	2.14×10^{-5}	6.3	6.87×10^{-6}	9.1	2.02×10^{-5}	9.98
Forward 4b	3.9	2.10×10^{-5}	6.5	6.81×10^{-6}	9.1	2.04×10^{-5}	8.08
Forward average	3.0 ± 0.1	$1.67\pm0.29\times10^{-5}$	6.5 ± 0.1	$5.61\pm0.87\times10^{-6}$	9.2 ± 0.1	$1.73\pm0.21\times10^{-5}$	
Reverse 1a	4.0	1.41×10^{-5}	6.6	4.98×10^{-6}	9.3	1.53×10^{-5}	6.02
Reverse 1b	4.0	1.37×10^{-5}	6.5	4.86×10^{-6}	9.2	1.53×10^{-5}	5.60
Reverse 2a	4.0	1.61×10^{-5}	6.5	5.42×10^{-6}	9.3	1.59×10^{-5}	7.39
Reverse 2b	4.0	1.53×10^{-5}	6.5	5.29×10^{-6}	9.3	1.57×10^{-5}	7.01
Reverse 3a	4.0	1.63×10^{-5}	6.5	6.24×10^{-6}	9.3	1.75×10^{-5}	8.68
Reverse 3b	4.1	1.55×10^{-5}	6.6	6.14×10^{-6}	9.3	1.77×10^{-5}	7.20
Reverse 4a	3.8	2.24×10^{-5}	6.3	7.16×10^{-6}	9.1	2.00×10^{-5}	8.78
Reverse 4b	3.7	2.27×10^{-5}	6.3	7.22×10^{-6}	9.1	2.03×10^{-5}	9.34
Reverse average	3.9 ± 0.1	$1.70\pm0.35\times10^{-5}$	6.5 ± 0.1	$5.91\pm0.93\times10^{-6}$	9.2 ± 0.1	$1.72\pm0.20\times10^{-5}$	
Combined average	4.0 ± 0.1	$1.68\pm0.31\times10^{-5}$	6.5 ± 0.1	$5.76\pm0.88\times10^{-6}$	9.2 ± 0.1	$1.73\pm0.20\times10^{-5}$	

from those calculated for the 0.01 and 0.1 M exudate solutions (e.g., for *B. subtilis*, $pK_{a(1)}$ is 4.5 ± 0.2 in 0.3 M but 3.9 ± 0.3 and 4.0 ± 0.2 in 0.01 and 0.1 M, respectively; for *S. oneidensis* $pK_{a(1)}$ is 4.3 ± 0.2 in 0.3 M but 3.7 ± 0.2 and 3.8 ± 0.2 in 0.01 and 0.1 M, respectively). However, these differences are only slightly outside the 1 σ error and, as they are still within the 2 σ error, combined averages from the three ionic strengths are still calculated and compared below.

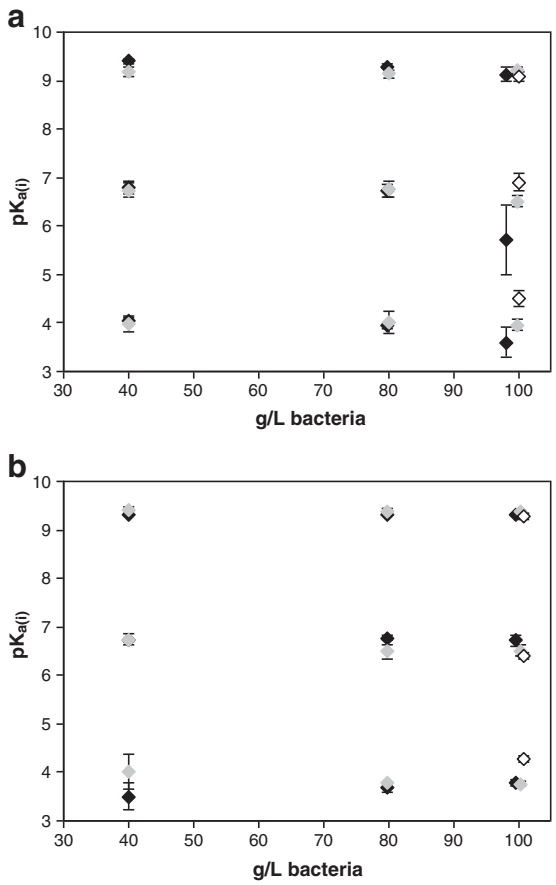

Fig. 6. Bacterial exudate $pK_{a(i)}$ values. Comparison of the calculated $pK_{a(i)}$ values for a) *B. subtilis* and b) *S. oneidensis* exudate solutions made using 40, 80, and 100 g/L bacterial concentrations and 0.01 (black), 0.1 (gray), or 0.3 (white) M $NaClO_4$.

Ionic strength exhibits a greater influence on the calculated site concentrations for the individual and total exudate sites than on the $pK_{a(i)}$ values (Figs. 7 and 8). For the *B. subtilis* exudate solutions, there is a decrease in the calculated site 1 concentrations with increasing ionic strength and only a very slight decrease with increasing ionic strength in the site 2 and 3 concentrations (Fig. 7a–c). The total site concentrations for the *B. subtilis* exudates decrease with increasing ionic strength from $7.62\pm1.60\times10^{-5}$ to $4.26\pm0.56\times10^{-5}$ to $2.76\pm0.40\times10^{-5}$ mol/g bacteria (wet weight) at 0.01, 0.1, and 0.3 M $NaClO_4$, respectively (Fig. 7d). Conversely, for *S. oneidensis*, the concentrations for sites 2 and 3 increase significantly with increasing ionic strength, with only a very slight increase in the site 1 concentrations (Fig. 8a–c). The total site concentrations in the *S. oneidensis* exudates increase with increasing ionic strength from $3.57\pm0.49\times10^{-5}$ to $6.05\pm0.50\times10^{-5}$ to $8.20\pm0.63\times10^{-5}$ mol/g bacteria (wet weight) at 0.01, 0.1, and 0.3 M $NaClO_4$, respectively (Fig. 8d).

Although, as we summarized above, some significant differences in site concentration exist as a function of ionic strength, the ionic strength dependence is not large for the exudates from either species, and reasonable estimates of proton binding can be attained over the ionic strength conditions, and initial bacterial concentrations, from a single averaged set of $pK_{a(i)}$ and site concentration values for both bacterial species. Table 3 lists these overall average values. The *B. subtilis* exudate has average $pK_{a(i)}$ values of 4.0 ± 0.3, 6.6 ± 0.5, and 9.2 ± 0.1, and the *S. oneidensis* exudate has average $pK_{a(i)}$ values of 3.9 ± 0.3, 6.6 ± 0.2, and 9.3 ± 0.1 (Table 3). Thus, the $pK_{a(i)}$ values for the exudates from the two bacterial species are not significantly different and can be averaged to yield combined $pK_{a(i)}$ values of 3.9 ± 0.3, 6.6 ± 0.4, and 9.3 ± 0.1. As mentioned previously, the exudates from the two bacterial species show opposite trends in their site concentrations with increasing ionic strength; however, their total site concentrations cover a similar range (roughly $2.8–8.2\times10^{-5}$ mol/g). Combined average site concentrations for the two bacterial species are $1.85\pm1.10\times10^{-5}$, $1.01\pm0.51\times10^{-5}$, and $2.82\pm1.10\times10^{-5}$ mol/g for sites 1, 2, and 3, respectively. The usefulness of the overall averaged model depends upon the specific purpose of the modeling: a laboratory-scale study with exudates from a single bacterial species may exhibit proton binding behavior significantly different from the averaged model; however, for modeling the behavior of exudates in an environmental system in which a range of bacterial species exist, the averaged calculated model parameters are likely to yield a reasonable estimation, in the absence of data specifically for the species present in the system.

The similarities in calculated $pK_{a(i)}$ values and site concentrations for the exudates of these two bacterial species are interesting given the

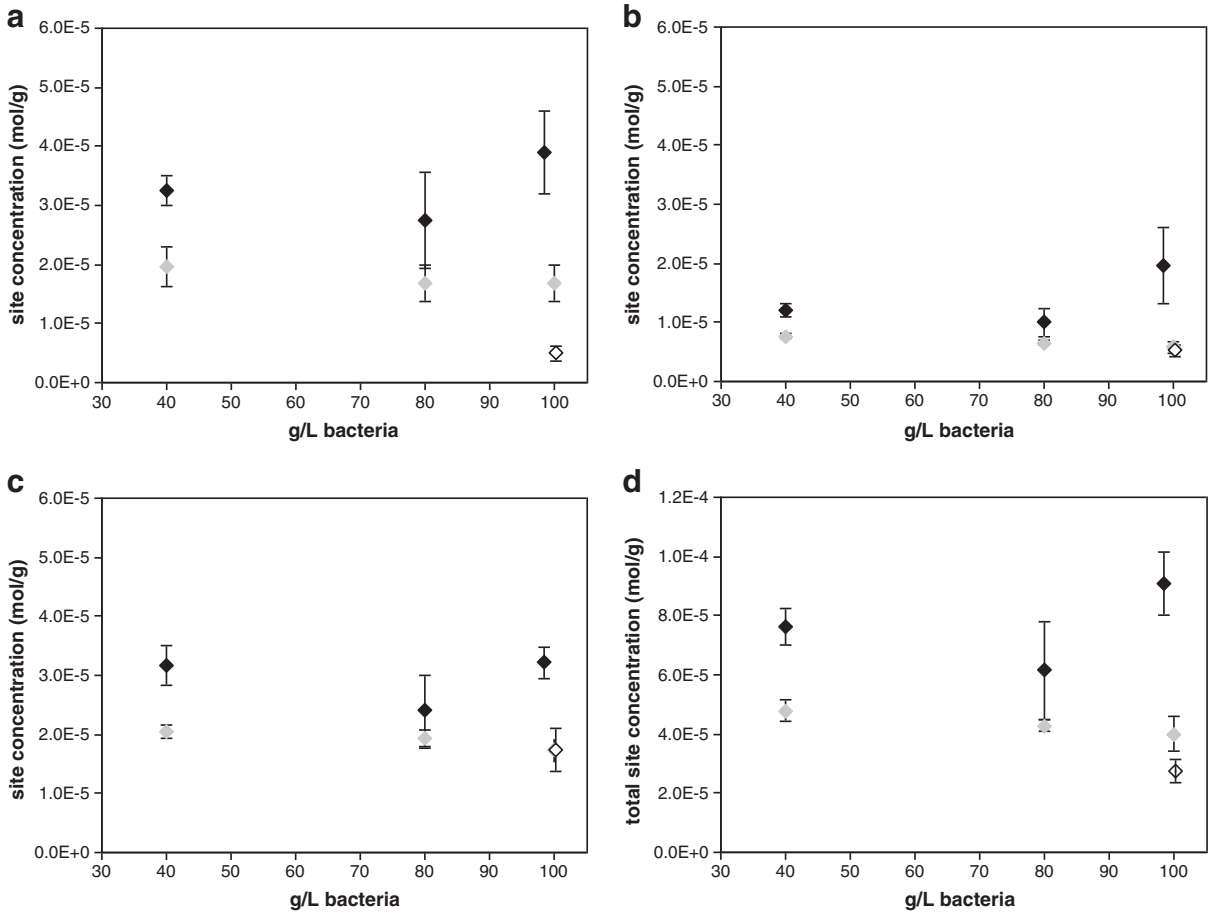

Fig. 7. *B. subtilis* exudate site concentrations. Comparison of the calculated site concentrations (moles of site per g bacteria) for *B. subtilis* exudates at a) site 1, b) site 2, c) site 3, and d) total sites from solutions with 40, 80, and 100 g/L initial bacterial concentrations and 0.01 M (black), 0.1 M (gray), or 0.3 M (white) $NaClO_4$.

differences in the cell wall structures of the bacteria that generated the exudates. Gram-positive bacteria, such as *B. subtilis*, have a framework of peptidoglycan shaping the cell wall with teichoic and/or teichuronic acid components joined to the peptidoglycan, whereas Gram-negative bacteria, such as *S. oneidensis*, have a peptidoglycan layer in their periplasm, which is covered by a lipopolysaccharide-phospholipid outer layer (e.g., Beveridge, 1989). However, in spite of these differences in cell wall structure, both the modeling and the FTIR data showed little difference in the exudates from the two bacterial species. It may be that the soluble organics, which likely include polysaccharides and DNA as suggested by the FTIR spectra, are similar for exudates from a range of bacterial species, leading to a 'universal' soluble fraction. This finding is similar to that of Borrok et al. (2005) which shows that a single set of 'universal' pK_a and site concentration values can be used to characterize the proton binding of a range of Gram-positive and Gram-negative bacteria, as well as a range of bacterial consortia (Borrok et al., 2005).

However, the bacterial exudates exhibit lower total site concentrations ($2.8–8.2\times10^{-5}$ mol/g with an average of $5.68\pm2.08\times10^{-5}$ mol/g) compared to the bacterial cells that produced them. For example, *B. subtilis* cells have total site concentrations of $1.75\pm0.24\times10^{-4}$, $3.19\pm0.16\times10^{-4}$, and $3.44\pm0.16\times10^{-4}$ mol/g in solutions of 0.01, 0.1, and 0.3 M $NaClO_4$, respectively (Borrok et al., 2005), which also show a trend of increasing values with increasing ionic strength as do the exudates studied here. The total site concentration for *S. oneidensis* cells in 0.1 M $NaClO_4$ is 3.9×10^{-4} mol/g (Mishra et al., 2010). Furthermore, the average total site concentration calculated from 36 sets of potentiometric titration data involving either bacterial species or bacterial consortia is $3.2\pm1.0\times10^{-4}$ mol/g (Borrok et al., 2005). Thus, the total site concentration for bacterial cells varies over a relatively small range, which is significantly higher than the range observed in this study for bacterial exudates. The total site concentrations for the exudates are closer to the total site concentrations calculated by Kaulbach et al. (2005) from the algal species *P. subcapitata* ($2.77\pm0.29\times10^{-5}$ mol/g).

The bacterial exudate titration data and model results were also normalized to g exudate per L and compared to data previously collected for a range of EPS samples and humic substances. Previous titrations of various EPS samples identified between two and six binding sites (Liu and Fang, 2002; Guibaud et al., 2005; Braissant et al., 2007; Baker et al., 2010) with total site concentrations ranging from 5.4 to 16.4×10^{-3} mol/g EPS (Liu and Fang, 2002; Braissant et al., 2007; Baker et al., 2010). The calculated average total site concentrations for the *B. subtilis* and the *S. oneidensis* exudates in 0.1 M $NaClO_4$ were $3.11\pm0.41\times10^{-3}$ mol/g and $9.61\pm0.79\times10^{-3}$ mol/g, respectively. Given the relatively large uncertainties associated with the determinations of total exudate mass in solution using our approach, the calculated exudate site concentrations are similar to those of EPS.

Similarities were also observed between the calculated total buffering capacities and total site concentrations of the bacterial exudates and those of humic substances. For example, the total buffering capacity from pH 4 to 9 of an aquatic humic acid collected from Whitray Beck (sample HH8 in Borrok and Fein, 2004) in a solution of approximately 0.1 M ionic strength is 3.0×10^{-3} mol/g humic acid (Lead et al., 1994). This value agrees within uncertainty with the total buffering capacities calculated from pH 4 to 9 for both types of exudate solutions in 0.1 M $NaClO_4$ and averaged for the three starting concentrations ($1.72\pm0.25\times10^{-3}$ mol/g exudate for *B. subtilis* exudates and $4.61\pm0.62\times10^{-3}$ mol/g exudate for *S. oneidensis* exudates). The combined average total site concentrations from potentiometric titration

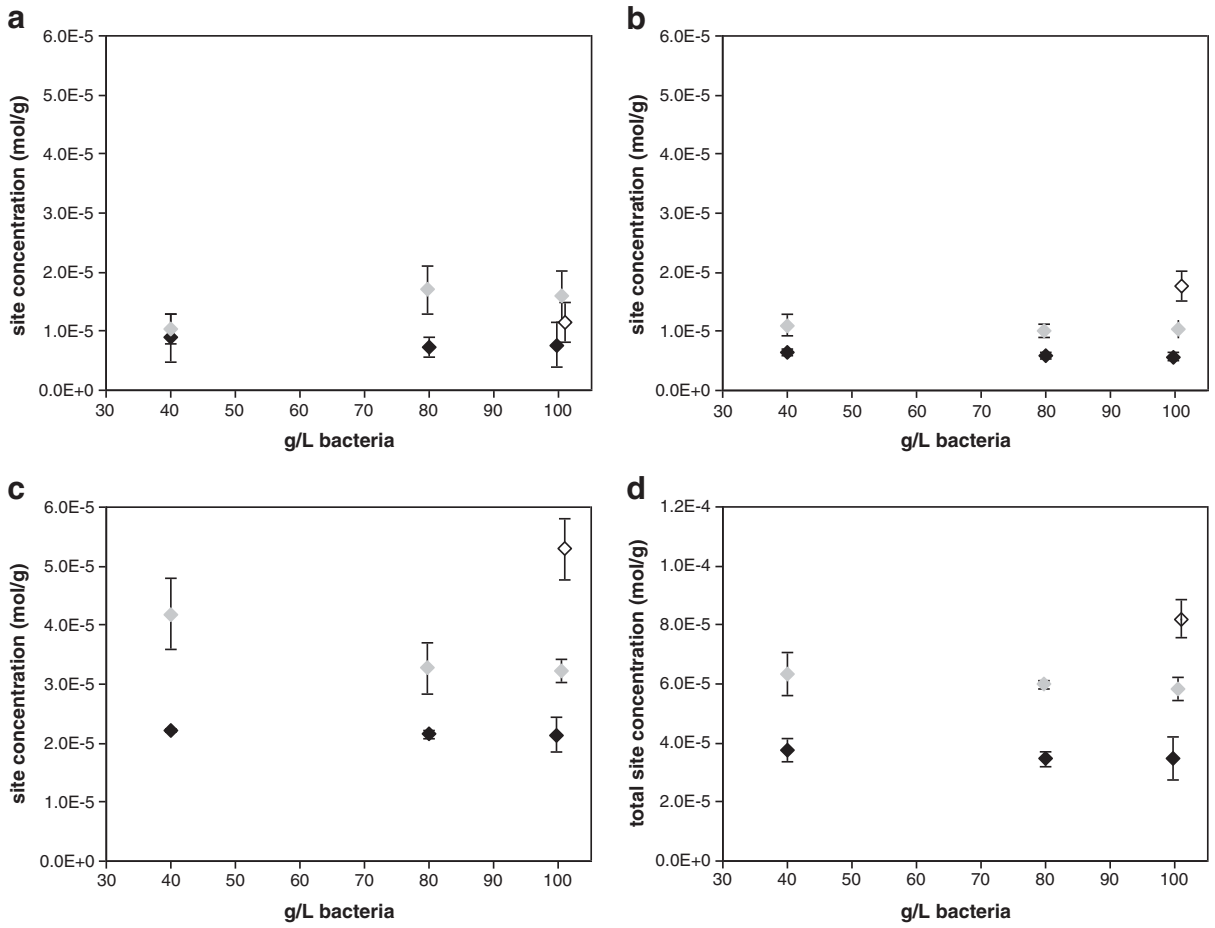

Fig. 8. *S. oneidensis* exudate site concentrations. Comparison of the calculated site concentrations (moles of site per g bacteria) for *S. oneidensis* exudates at a) site 1, b) site 2, c) site 3, and d) total sites from solutions with 40, 80, and 100 g/L initial bacterial concentrations and 0.01 M (black), 0.1 M (gray), or 0.3 M (white) $NaClO_4$.

data of 8 humic acids and 9 fulvic acids in approximately 0.1 M ionic strength solutions calculated by Borrok and Fein (2004) is $4.90 \pm 1.07 \times 10^{-3}$ mol/g humic substance, a value that agrees within uncertainty with that calculated for the *B. subtilis* exudates ($3.11 \pm 0.41 \times 10^{-3}$ mol/g) and the *S. oneidensis* exudates ($9.61 \pm 0.79 \times 10^{-3}$ mol/g) in 0.1 M $NaClO_4$. The similarity between the total site concentrations of these humic and fulvic acids and the bacterial exudates probably arises due to similarities in component organic acids present in the bacterial exudates and the humic substances, and in fact bacterial exudates may be constituents or precursors of humic substances (e.g., Visser, 1983; Aiken et al., 1985; Stumm and Morgan, 1996; Kördel et al., 1997). Based upon the similarities between the total buffering capacities and site concentrations for the humic substances and bacterial exudates, it may be that the tendencies of humic substances and bacterial exudates to bind with aqueous metal cations are also similar.

4. Conclusions

Potentiometric titrations and chemical equilibrium modeling were used to characterize the proton binding of bacterial exudates from *B. subtilis* and *S. oneidensis* bacterial cells. The calculated total buffering capacity of the bacterial exudates decreases with increasing ionic strength for the *B. subtilis* exudates but increases for the *S. oneidensis* exudates. Total site concentrations, which are likely related to buffering capacity, also change with ionic strength following the same trends as the buffering capacities. Calculated $pK_{a(i)}$ values and FTIR spectra, however, do not vary significantly as a function of ionic strength or bacterial type and concentration.

The total site concentrations calculated for the bacterial exudate solutions are approximately an order of magnitude lower per gram of bacteria than those calculated previously for a range of bacterial species. These differences suggest that exudates, with their lower site concentrations, are less efficient at binding protons and metals than bacterial surfaces per gram of bacteria. However, bacterial exudates exhibit remarkably similar proton binding capacities to humic substances. This similarity suggests that exudates may be a component or a precursor to these humic materials, and that binding constants for protons and metals with both exudates and humic and fulvic acids may be similar as well. The concentrations and distribution of bacterial exudates in the environment are not well established, and they may

Table 3
Calculated $pK_{a(i)}$ values and site concentrations (mol/g) averaged for all initial bacterial concentrations and ionic strengths for *B. subtilis* exudates, *S. oneidensis* exudates, and the two types of exudates combined.

	$pK_{a(1)}$	[Site 1]	$pK_{a(2)}$	[Site 2]	$pK_{a(3)}$	[Site 3]	Total sites
B. subtilis exudate	4.0 ± 0.3	$2.40 \pm 1.12 \times 10^{-5}$	6.6 ± 0.5	$9.96 \pm 5.44 \times 10^{-6}$	9.2 ± 0.1	$2.39 \pm 0.71 \times 10^{-5}$	$5.79 \pm 2.23 \times 10^{-5}$
S. oneidensis exudate	3.9 ± 0.3	$1.13 \pm 0.48 \times 10^{-5}$	6.6 ± 0.2	$1.03 \pm 0.46 \times 10^{-5}$	9.3 ± 0.1	$3.38 \pm 1.27 \times 10^{-5}$	$5.53 \pm 1.86 \times 10^{-5}$
Exudates combined	3.9 ± 0.3	$1.85 \pm 1.10 \times 10^{-5}$	6.6 ± 0.4	$1.01 \pm 0.51 \times 10^{-5}$	9.3 ± 0.1	$2.82 \pm 1.10 \times 10^{-5}$	$5.68 \pm 2.08 \times 10^{-5}$

constitute a significant portion of the proton and metal binding capacity of the aqueous phase, especially in bacteria-rich systems such as soils. The study of the effects and characteristics of bacterial exudates is in its infancy. These molecules can affect metal reduction, metal binding, and mineral dissolution rates, and the binding properties determined in this study provide a framework for understanding the mechanisms of how bacterial exudates interact with other components in geologic and engineered systems.

Acknowledgements

The authors would like to thank J. Szymanowski for assistance with the experimental data collection and E.A. Haack for the help in interpreting the FTIR data. Thanks also go to the Center for Environmental Science and Technology and its staff for providing instrumentation and technical support. Funding for this research was provided by an Environmental Molecular Science Institute grant to University of Notre Dame (EAR02-21966). Two thorough journal reviews are appreciated and significantly improved the presentation of the research.

Appendix A. Supplementary data

Supplementary data to this article can be found online at doi:10.1016/j.chemgeo.2011.03.017.

References

Aiken, G.R., McKnight, D.M., Wershaw, R.L., MacCarthy, P. (Eds.), 1985. Humic Substances in Soil, Sediment, and Water. Wiley-Interscience, New York, p. 692.

Baker, M.G., Lalonde, S.V., Konhauser, K.O., Foght, J.M., 2010. Role of extracellular polymeric substances in the surface chemical reactivity of *Hymenobacter aerophilus*, a psychrotolerant bacterium. Applied and Environmental Microbiology 76 (1), 102–109.

Bennett, P.C., Rogers, J.R., Choi, W.J., Hiebert, F.K., 2001. Silicates, silicate weathering, and microbial ecology. Geomicrobiology Journal 18, 3–19.

Beveridge, T.J., 1989. Role of cellular design in bacterial metal accumulation and mineralization. Annual Reviews in Microbiology 43, 147–171.

Beveridge, T.J., Murray, R.G.E., 1976. Uptake and retention of metals by cell walls of *Bacillus subtilis*. Journal of Bacteriology 127, 1502–1518.

Beveridge, T.J., Murray, R.G.E., 1980. Sites of metal deposition in the cell wall of *Bacillus subtilis*. Journal of Bacteriology 141, 876–887.

Borch, T., Kretzschmar, R., Kappler, A., van Cappellen, P., Ginder-Vogel, M., Voegelin, A., Campbell, K., 2010. Biogeochemical redox processes and their impact on contaminant dynamics. Environmental Science and Technology 44 (1), 15–23.

Borrok, D., Fein, J.B., 2004. Distribution of protons and Cd between bacterial surfaces and dissolved humic substances determined through chemical equilibrium modeling. Geochimica et Cosmochimica Acta 68 (14), 3043–3052.

Borrok, D., Turner, B.F., Fein, J.B., 2005. A universal surface complexation framework for modeling proton binding onto bacterial surfaces in geologic settings. American Journal of Science 305 (6–8), 826–853.

Braissant, O., Decho, A.W., Dupraz, C., Glunk, C., Przekop, K.M., Visscher, P.T., 2007. Exopolymeric substances of sulfate-reducing bacteria: interactions with calcium at alkaline pH and implication for formation of carbonate minerals. Geobiology 5, 401–411.

Brandenburg, K., Seydel, U., 1996. Fourier transform infrared spectroscopy of cell surface polysaccharides. In: Mantsch, H.H., Chapman, D. (Eds.), Infrared Spectroscopy of Biomolecules. Wiley-Liss, New York, pp. 203–237.

Brown Jr., G.E., Parks, G.A., 2001. Sorption of trace elements on mineral surfaces: modern perspectives from spectroscopic studies, and comments on sorption in the marine environment. International Geology Review 43 (11), 963–1073.

Fein, J.B., Boily, J.-F., Yee, N., Gorman-Lewis, D., Turner, B.F., 2005. Potentiometric titrations of *Bacillus subtilis* cells to low pH and a comparison of modeling approaches. Geochimica et Cosmochimica Acta 69 (5), 1123–1132.

Fortin, D., Beveridge, T.J., 1997. Role of the bacterium *Thiobacillus* in the formation of silicates in acidic mine tailings. Chemical Geology 141, 235–250.

Guibaud, G., Comte, S., Bordas, F., Dupuy, S., Baudu, M., 2005. Comparison of the complexation potential of extracellular polymeric substances (EPS), extracted from activated sludges and produced by pure bacteria strains, for cadmium, lead and nickel. Chemosphere 59, 629–638.

Ha, J., Gélabert, A., Spormann, A.M., Brown Jr., G.E., 2010. Role of extracellular polymeric substances in metal ion complexation on *Shewanella oneidensis*: batch uptake, thermodynamic modeling, ATR-FTIR, and EXAFS study. Geochimica et Cosmochimica Acta 74, 1–15.

Haris, P.I., Chapman, D., 1996. Fourier transform infrared spectroscopic studies of biomembrane systems. In: Mantsch, H.H., Chapman, D. (Eds.), Infrared Spectroscopy of Biomolecules. Wiley-Liss, New York, pp. 239–278.

Jiang, W., Saxena, A., Song, B., Ward, B.B., Beveridge, T.J., Myneni, S.C.B., 2004. Elucidation of functional groups on Gram-positive and Gram-negative bacterial surfaces using infrared spectroscopy. Langmuir 20 (26), 11433–11442.

Kaulbach, E.S., Szymanowski, J.E.S., Fein, J.B., 2005. Surface complexation modeling of proton and Cd adsorption onto an algal cell wall. Environmental Science and Technology 39 (11), 4060–4065.

Kördel, W., Dassenakis, M., Lintelmann, J., Padberg, S., 1997. The importance of natural organic material for environmental processes in waters and soils. Pure and Applied Chemistry 69 (7), 1571–1600.

Lead, J.R., Hamilton-Taylor, J., Hesketh, N., Jones, M.N., Wilkinson, A.E., Tipping, E., 1994. A comparative study of proton and alkaline earth metal binding by humic substances. Analytica Chimica Acta 294, 319–327.

Lee, J.-U., Fein, J.B., 2000. Experimental study of the effects of *Bacillus subtilis* on gibbsite dissolution rates under near-neutral pH and nutrient-poor conditions. Chemical Geology 166, 193–202.

Liu, H., Fang, H.H.P., 2002. Characterization of electrostatic binding sites of extracellular polymers by linear programming analysis of titration data. Biotechnology and Bioengineering 80 (7), 806–811.

Lovely, D.R., 1993. Dissimilatory metal reduction. Annual Reviews in Microbiology 47, 263–290.

NIST critically selected stability constants of metal complexes. In: Martell, A.E., Smith, R.M. (Eds.), NIST Standard Reference Database 46, Version 6.0.

Mishra, B., Boyanov, M., Bunker, B.A., Kelly, S.D., Kemner, K.M., Fein, J.B., 2010. High- and low-affinity binding sites for Cd on the bacterial cell walls of *Bacillus subtilis* and *Shewanella oneidensis*. Geochimica et Cosmochimica Acta 74, 4219–4233.

Mrozik, A., Piotrowska-Seget, Z., 2010. Bioaugmentation as a strategy for cleaning up of soils contaminated with aromatic compounds. Microbiological Research 165, 363–375.

Naumann, D., Schultz, C.P., Helm, D., 1996. What can infrared spectroscopy tell us about the structure and composition of intact bacterial cells? In: Mantsch, H.H., Chapman, D. (Eds.), Infrared Spectroscopy of Biomolecules. Wiley-Liss, New York, pp. 279–310.

Newman, D.K., Banfield, J.F., 2002. Geomicrobiology: how molecular-scale interactions underpin biogeochemical systems. Science 296, 1071–1077.

Ohnuki, T., Yoshida, T., Ozaki, T., Kozai, N., Sakamoto, F., Nankawa, T., Suzuki, Y., Francis, A.J., 2007. Chemical speciation and association of plutonium with bacteria, kaolinite clay, and their mixture. Environmental Science and Technology 41 (9), 3134–3139.

Perry, T.D., McNamara, C.J., Mitchell, R., Hernandez-Duque, G., 2003. An investigation of bacterial dissolution of Maya limestone: biodiversity and functional analysis. Molecular Biology and Cultural Heritage 137–140.

Perry IV, T.D., Klepac-Ceraj, V., Zhang, X.V., McNamara, C.J., Polz, M.F., Martin, S.T., Berke, N., Mitchell, R., 2005. Binding of harvested bacterial exopolymers to the surface of calcite. Environmental Science and Technology 39 (22), 8770–8775.

Pokrovsky, O.S., Shirokova, L.S., Bénézeth, P., Schott, J., Golubev, S.V., 2009. Effect of organic ligands and heterotrophic bacteria on wollastonite dissolution kinetics. American Journal of Science 309, 731–772.

Stumm, W., Morgan, J.J., 1996. Aquatic Chemistry. Wiley-Interscience, New York, p. 1022.

Tiquia, S.M., 2010. Salt-adapted bacteria isolated from the Rouge River and potential for degradation of contaminants and biotechnological applications. Environmental Technology 31 (8–9), 967–978.

Venkateswaran, K., Moser, D.P., Dollhopf, M.E., Lies, D.P., Saffarini, D.A., MacGregor, B.J., Ringelberg, D.B., White, D.C., Nishijima, M., Sano, H., Burghardt, J., Stackebrandt, E., Nealson, K.H., 1999. Polyphasic taxonomy of the genus *Shewanella* and description of *Shewanella oneidensis* sp. nov. International Journal of Systematic Bacteriology 49 (2), 705–724.

Visser, S.A., 1983. Application of van Krevelen's graphical-statistical method for the study of aquatic humic material. Environmental Science and Technology 17 (7), 412–417.

Westall, J.C., 1982. FITEQL, a computer program for determination of chemical equilibrium constants from experimental data. Version 2.0. Report 82-02, Dept. of Chemistry, Oregon State Univ., Corvallis, Oregon.

Westall, J.C., Jones, J.D., Turner, G.D., Zachara, J.M., 1995. Models for association of metal ions with heterogeneous environmental sorbents. 1. Complexation of Co(II) by Leonardite humic acid as a function of pH and $NaClO_4$ concentration. Environmental Science and Technology 29 (4), 951–959.

Yang, L., Zhang, L.-M., 2009. Chemical structural and chain conformational characterization of some bioactive polysaccharides isolated from natural sources. Carbohydrate Polymers 76, 349–361.

Young, K.C., Docherty, K.M., Maurice, P.A., Bridgham, S.D., 2005. Degradation of surface-water dissolved organic matter: influences of DOM chemical characteristics and microbial populations. Hydrobiologia 539, 1–11.